

Compact Gravity Wave Detector

Munawar Karim

Department of Physics, St. John Fisher College, Rochester, NY 14618

(Dated:)

Abstract

Using a combination of analogue and digital signal processing techniques we show how a compact interferometer can be made sensitive to gravity wave amplitudes of 10^{-22} . As an example we describe a 10cm Michelson interferometer designed to measure gravity waves from sources as far as the Virgo cluster.

I.

II. INTRODUCTION

Following earlier attempts by Weber [1], Forward [2] and Weiss [3], several groups have been engaged in building detectors and observatories to study gravitational radiation from astrophysical sources. Among those which seem most likely to emit signals strong enough and often enough to trigger current detectors are inspiralling binary neutron stars from distances up to the Virgo cluster.

Detectors may be classified as either resonant mass or interferometric. We will be concerned with the latter only.

Interferometric detectors rely on detecting relative phase changes between a pair of mutually orthogonal light beams intersecting a pulse of gravitational radiation. Interference patterns jiggle because of momentary differences in the time-delay caused by metric perturbations due to a pulse of a passing gravity wave.

A. Sensitivity Calculations

The interferometer arms are aligned along the x - and y -axes. The arms are of length L as measured in flat space. The gravitational wave described by a four-vector $k_\rho = (\omega, \mathbf{k})$, which is incident along the z -axis, perturbs the metric by a small amplitude. The background is a flat metric ($\eta_{\mu\nu}$); the perturbed metric is:

$$g_{\mu\nu} = \eta_{\mu\nu} + h_{\mu\nu} \quad (1)$$

A null vector represents light in the interferometer. Because of the x - and y -alignment of the arms we need consider only the (11) and (22) components of the metric: the beam splitter and mirrors are in free fall.

$$ds^2 = 0 = g_{\mu\nu} dx^\mu dx^\nu = (\eta_{\mu\nu} + h_{\mu\nu}) dx^\mu dx^\nu \quad (2)$$

$$0 = -c^2 dt^2 + [1 + h_{11}(\omega t - \mathbf{k} \cdot \mathbf{x})] dx^2 \quad (3)$$

The gravity wave affects both time and space components. The coordinate length L is altered to proper length $L_x = L + \xi^1$ (Eq.(7)). Along the x -axis the round-trip light travel time is:

$$\tau_{rt} = \frac{2L_x}{c} + \frac{1}{2c} \int_0^{L_x} h_{11}(\omega t - \mathbf{k} \cdot \mathbf{x}) dx - \frac{1}{2c} \int_{L_x}^0 h_{11}(\omega t - \mathbf{k} \cdot \mathbf{x}) dx \quad (4)$$

A similar integral appears for the y -axis with h_{22} substituted for h_{11} and the limit $L_y = L + \xi^2$. In the transverse traceless gauge we are working with $h = h_{11} = -h_{22}$; the arm lengths are affected in opposite directions. h is assumed to be constant over the range of the integral.

The integrals may be evaluated to obtain the difference in round-trip travel times between the x - and y -axes. The time difference is:

$$\Delta\tau_i = 2 \frac{\xi^1 - \xi^2}{c} + h(t) \frac{2L_i}{c} = 2 \frac{\xi^1 - \xi^2}{c} + h(t) \tau_i \quad (5)$$

where τ_i is the proper round-trip time for the i -th beam traversing the interferometer:

$$\tau_i = 2 \left[\frac{L_x + L_y}{c} \right] = \frac{2L_i}{c} \quad (6)$$

obtained after substituting $h_{11} = -h_{22}$ in Eq.(7). A general reference for this discussion is Saulson [4].

In the interferometer we are describing, independent light beams traverse the interferometer several times. Each round-trip accrues a time delay of $\Delta\tau_i$; for p -round-trips the time delay is $p\Delta\tau_i$ (for a constant h , since $\Delta\tau_i \ll$ duration of the gravity wave pulse, this is a reasonable assumption). Each sample is τ_i in duration. This method of sampling requires identification of the i -th beam. The interference intensity is recorded in discrete samples.

The metric of the incident gravity wave has intrinsic curvature (non-zero Riemann tensor), implying a wave-front surface that is saddle-like (fig.1). The time delay $\Delta\tau_i$ may be interpreted as the excess angle $\Delta\phi_i$ acquired by a null-vector (light beam) parallel transported simultaneously along two closed loops (x - and y -axes), on a surface with intrinsic curvature (fig.1).

1. Response of interferometer and mirror mount

The interferometer responds to the incident gravity wave. The interferometer is a rigid platform. It is accelerating upwards to counter Earth's gravity. It is in principle not in an inertial frame. Acceleration, in principle, affects both mirror spacing and time delay. These effects are taken care of by equations of special relativity. For a detailed discussion and experimental confirmation see [9],[10]. For a system accelerating $@g \approx 10m/\text{sec}^2$, times and lengths will change according to [8]:

$$t = t_0 + (c/g) \sinh(g\tau/c) \quad \text{and} \quad x = x_0 + (c^2/g) [\cosh(g\tau/c) - 1]$$

For measurement intervals $\tau \ll 1$ secs there is negligible change in either t or x . Acceleration is not an issue, the platform is in practice, inertial.

What is the effect of the rigid platform? The time delay Eq.(5) is the sum of contributions from time and space components.

Since the phase of a plane wave is an invariant quantity i.e., $\phi = \omega t - \mathbf{k} \cdot \mathbf{x} = \omega' t' - \mathbf{k}' \cdot \mathbf{x}'$, a change in phase in general stems from a change in both the time and space components. The gravity wave has two independent effects; (i) it alters clock rates (ii) it affects lengths. Just as the gravity wave changes the time delay from $\tau_i \rightarrow \tau_i + h\tau_i$, so does it alter the length $2L \rightarrow 2L + h2L$ (Eq.(7)). A quick way to see why there are two independent sources of the phase is to follow the world lines of the light rays emerging from the beam-splitter as they reflect off the two mirrors (fig.2). The mirrors are shown in two configurations: (i) in free fall and (ii) attached rigidly to the interferometer. In the frame of the platform the limits of the integrals in Eq.(4) are changed from 0 to L to 0 to $L + \xi^1$ and 0 to $L + \xi^2$ along the x - and y - axes respectively. The mirrors appear displaced in the same sense (as they must be for the ratio to be c , the speed of light measured by local observers) as in the freely falling case, but less so in the case of rigid mounts. In either case, whether in free fall or rigidly attached, there is still a phase difference because of the intrinsic curvature in the wave-front surface. Time and space components are affected independently. A quantitative discussion follows.

In the initial calculation the beam-splitter and mirrors were treated as test masses in free fall. Thus mirrors and beam-splitter move along individual geodesics. The calculations go like this: $\Delta\tau$ measures the difference in light travel times between the beam splitter and mirrors in free fall. However, measurements are made using rigid rulers in a non-inertial laboratory. In this laboratory one of the mirrors, of mass m is instantaneously at rest at a coordinate x^j with origin at the beam-splitter. The waves produce small oscillations of the test mass of amplitude ξ^j . The wave is so weak that $\xi^j \ll x^j$ thus x^k is essentially constant. The equation of motion is:

$$m \frac{\partial^2 \xi^j}{\partial t^2} = -m R_{j0k0}^{GW} x^k = -m \left[-\frac{1}{2} \frac{\partial^2 \tilde{h}_{jk}}{\partial t^2} \right] x^k$$

Integration gives [7]

$$\xi^j = \frac{1}{2} \tilde{h}_{jk} x^k \quad (7)$$

When \tilde{h}_{jk} is time-varying as is the case for gravity waves. One can calculate the response as follows: Consider the mirrors as test masses connected through a spring of length L , force constant k_α^μ with damping constant b_α^μ . The interferometer is in free fall. We may use geodesic coordinates where the Christoffel symbols are made zero [8] on all points on the geodesic. The geodesic is the world line of the beam-splitter. The time coordinate is along the instantaneous tangent to the world line of the beam-splitter. There is an orthogonal co-moving coordinate with the mirror lying on the x -axis. The quantities ($h_\alpha^\mu = h$, $k_\alpha^\mu = k$, $b_\alpha^\mu = b$) have only one component. The equation of motion which describes the mirror of mass m that has an instantaneous position x^1 is [1], with modifications:

$$\begin{aligned} \frac{\partial^2 x^1}{\partial t^2} + \frac{b}{m} \frac{\partial x^1}{\partial t} + \omega_0^2 (x^1 - L) &= -R_{1010}^{GW} x^1 = \frac{1}{2} \frac{\partial^2 \tilde{h}_{11}}{\partial t^2} x^1 = -\frac{1}{2} \omega^2 x^1 \tilde{h}_{11} \\ \frac{\partial^2 x^1}{\partial t^2} + \frac{b}{m} \frac{\partial x^1}{\partial t} + (\omega_0^2 + \frac{1}{2} \omega^2 h_{11} \sin \omega t) x^1 &= \omega_0^2 L \end{aligned} \quad (8)$$

where $\tilde{h}_{jk} = h_{jk} \sin \omega t$ and the fundamental mode is $\omega_0^2 \equiv k/m$; L is the relaxed length of the spring. This is an inhomogeneous Mathieu equation (for $b = 0$). What we observe here is that, under the action of the gravity wave, the mirror oscillates with a frequency that varies sinusoidally with a frequency-dependent amplitude of $O(h)$.

Eq.(8) says that the elastic properties of the mirror suspension, whether "soft" or rigid, depending as they do on the speed of sound and therefore on lengths and time, are modulated by the incident gravity wave.

We solve this equation for $Q \equiv \omega_0 m/b \gg 1$ or $(b/m) \ll 1$.

$$\frac{\partial^2 x^1}{\partial t^2} + (\omega_0^2 + \frac{1}{2} \omega^2 h_{11} \sin \omega t) x^1 = \omega_0^2 L$$

With initial conditions $x^1(0) = \frac{\partial x^1}{\partial t}(0) = 0$, to $O(h)$, the solution of Eq.(8) is [11]

$$\frac{x^1}{L} \approx L - \frac{1}{2} h_{11} \frac{\omega^2}{\omega_0 (\omega_0^2 - \omega^2)} (\omega_0 \sin \omega t - \omega \sin \omega_0 t); \omega \neq \omega_0 \quad (9)$$

For the mirror on the y -axis there is a similar equation:

$$\frac{\partial^2 x^2}{\partial t^2} + (\omega_0^2 + \frac{1}{2}\omega^2 h_{22} \sin \omega t)x^2 = \omega_0^2 L \quad (10)$$

with a similar solution:

$$\frac{x^2}{L} \approx L - \frac{1}{2}h_{22} \frac{\omega^2}{\omega_0(\omega_0^2 - \omega^2)} (\omega_0 \sin \omega t - \omega \sin \omega_0 t); \omega \neq \omega_0$$

The difference is, with $h = h_{11} = -h_{22}$:

$$\frac{x^1 - x^2}{L} = \frac{\xi^1 - \xi^2}{L} = h \frac{\omega^2}{\omega_0(\omega_0^2 - \omega^2)} (\omega_0 \sin \omega t - \omega \sin \omega_0 t); \omega \neq \omega_0$$

Substitution into Eq.(5) gives

$$\Delta\tau_i = \tau_i h \left(1 + \frac{\omega^2 (\omega_0 \sin \omega t - \omega \sin \omega_0 t)}{\omega_0 (\omega_0^2 - \omega^2)} \right); \omega \neq \omega_0 \quad (11)$$

for each traverse. For p independent samples the total excess time is:

$$p\Delta\tau_i = p\tau_i h \left(1 + \frac{\omega^2 (\omega_0 \sin \omega t - \omega \sin \omega_0 t)}{\omega_0 (\omega_0^2 - \omega^2)} \right); \omega \neq \omega_0 \quad (12)$$

Time and space contributions add in phase because the speed of sound in the platform material, sapphire is $\approx 10^4$ m/sec; the mirrors respond almost instantaneously i.e., within $0.10\text{m}/10^4\text{m/s} = 10\mu\text{sec}$, much less than the period $1/800\text{sec}$. The time delay can be related to the phase difference in monochromatic light beams of wavelength λ :

$$\Delta\phi_i = \Delta\tau_i \frac{2\pi c}{\lambda} \quad (13)$$

The total phase difference is the sum of the time and space contributions. Substituting into Eqs.(5,13)

$$\Delta\phi_i = \tau_i h \frac{2\pi c}{\lambda} + 2 \frac{\xi^1 - \xi^2}{c} \frac{2\pi c}{\lambda} = \tau_i h \frac{2\pi c}{\lambda} \left(1 + \frac{\omega^2 (\omega_0 \sin \omega t - \omega \sin \omega_0 t)}{\omega_0 (\omega_0^2 - \omega^2)} \right); \omega \neq \omega_0 \quad (14)$$

This is the phase-shift for each pass through the interferometer. For p independent passes the accumulated phase is

$$\Delta\phi = \sum_{i=1}^p \Delta\phi_i = p\Delta\phi_i = p\tau_i h \frac{2\pi c}{\lambda} \left(1 + \frac{\omega^2 (\omega_0 \sin \omega t - \omega \sin \omega_0 t)}{\omega_0 (\omega_0^2 - \omega^2)} \right); \omega \neq \omega_0 \quad (15)$$

For a stiff mount, which is more practical given the problems of vibration isolation, one may choose a high fundamental mode. For example if $\omega_0 = 2\pi \times 10^4$, and for a maximum driving frequency $\omega = 2\pi \times 800$, the second term is of order unity; the phase difference is almost entirely due to time component of the metric perturbation. There is an acceptable reduction in strain amplitude in exchange for ease in vibration isolation.

As mirror mounts are a major obstacle in interferometric detectors, being able to mount them in rigid platforms alleviates many problems, including noise due to Brownian motion.

The interferometer has an input and an output port. The laser power at these ports is P_{in} and P_{out} respectively. The minimum sensitivity depends, among other factors, on fluctuations of the average photon number. The average photon flux is:

$$\bar{n} = \frac{P_{out}}{\hbar \frac{2\pi c}{\lambda}} = \frac{P_{out} \lambda}{2\pi \hbar c} \text{ sec}^{-1} \quad (16)$$

The fluctuations in the average number of photons $\bar{N} = \bar{n}\tau$ is:

$$\frac{\sigma_{\bar{N}}}{\bar{N}} = \frac{1}{\sqrt{\bar{n}\tau_i}}$$

Under operating conditions where the mean power at the output port of the interferometer averaged over one circuit time interval is half the mean power at the input port, i.e.,

$$P_{out} = \frac{1}{2}P_{in} \quad (17)$$

Also:

$$\frac{dP_{out}}{d\tau} = \frac{dP_{out}}{dL} \frac{dL}{d\tau} = \frac{2\pi c}{\lambda} P_{in}$$

Each round-trip acquires a time uncertainty of:

$$\sigma_{\delta\tau}^i = \frac{\sigma_{\bar{N}}}{\bar{N}} / \frac{1}{P_{out}} \frac{dP_{out}}{d\tau} = \frac{1}{\sqrt{\bar{n}\tau_i}} \frac{2\lambda}{2\pi c} = \pm \sqrt{\frac{2\hbar\lambda}{P_{in}\pi c\tau_i}}$$

For p independent round-trips the time uncertainty is:

$$\sigma_{\delta\tau} = \pm \sqrt{\frac{2\hbar\lambda}{P_{in}\pi c\tau_i}} \sqrt{\frac{1}{p}} \quad (18)$$

For a shot-noise limited detector the sensitivity is obtained by equating this to the excess time delay Eq.(12):

$$\sigma_{\delta\tau} = \sqrt{\frac{2\hbar\lambda}{P_{in}\pi c p \tau_i}} = p\tau_i h \left(1 + \frac{\omega^2 (\omega_0 \sin \omega t - \omega \sin \omega_0 t)}{\omega_0 (\omega_0^2 - \omega^2)} \right); \omega \neq \omega_0$$

The equivalent minimum detectable metric perturbation for a laser with wavelength λ is:

$$h \geq \left(\frac{1}{p\tau_i} \right)^{3/2} \sqrt{\frac{2\hbar\lambda}{P_{in}\pi c}} \left(1 + \frac{\omega^2 (\omega_0 \sin \omega t - \omega \sin \omega_0 t)}{\omega_0 (\omega_0^2 - \omega^2)} \right)^{-1}; \omega \neq \omega_0$$

This expression assumes that shot noise is dominant; Brownian noise and radiation pressure noise are negligible; generally true for the example under consideration.

III. DETECTION SCHEME

A. Over-sampled detector

The expected signal is a pulse of duration $\tau \sim 10\text{ms}$ of $h \sim 10^{-21}$ centered at a frequency of $\sim 800\text{Hz}$.

We can choose a sampling frequency. Generally, the minimum sampling frequency, called the Nyquist frequency, is twice the bandwidth of the signal to be sampled. For example, a signal with a bandwidth of 100Hz need be sampled every 200Hz, under ideal conditions, to be reproduced flawlessly. Practical considerations dictate the technique of "over-sampling", that is, sampling at rates which are integer multiples of the Nyquist frequency. The original signal is reproduced from sampled segments.

Light from a laser enters a Michelson interferometer. It passes through a beam-splitter, reflects off two mirrors onto a photodiode where the interference intensity is recorded (fig.3); the beam exits the interferometer. The averaged intensity is that of the i -th sample. The photodiode output is averaged over an interval τ_i . Each sample is independent. τ_i is the round-trip travel time for the i -th beam; it is also the optimum sampling interval.

The over-sampling frequency is $f_S \sim GHz$ for the example we will describe, compared with the signal bandwidth $f_B = 800Hz$. Thus the over-sampling frequency is 10^6 times the Nyquist frequency.

We give an example of what can be achieved in an $L_i = 10cm$ Michelson interferometer. Using a 1 watt light source of wavelength $0.545\mu m$, and sampling every $\tau_i = (2L_i/c) = (2/3) \times 10^{-9}$ secs.

Since the duration of the pulse is expected to be 10^{-2} secs, the product $p\tau_i = 10^{-2}$ secs. One may collect as many as 1.5×10^7 discrete samples if we choose to integrate over the entire length of the pulse. The sensitivity is:

$$h \geq \left(\frac{1}{p\tau_i} \right)^{3/2} \sqrt{\frac{2\hbar\lambda}{P_{in}\pi c}} \left(1 + \frac{\omega^2(\omega_0 \sin \omega t - \omega \sin \omega_0 t)}{\omega_0(\omega_0^2 - \omega^2)} \right)^{-1} \quad (19)$$

$$h \geq 10^{-22} \left(1 + \frac{\omega^2(\omega_0 \sin \omega t - \omega \sin \omega_0 t)}{\omega_0(\omega_0^2 - \omega^2)} \right)^{-1}; \omega \neq \omega_0 \quad (20)$$

$$h \geq 10^{-22} \quad (21)$$

a result which depends only on the pulse duration but is noticeably independent of the sampling interval τ_i , and necessarily, the length L_i . The equivalent length of the interferometer is $1500km$, half the distance a light beam travels during the $10m$ sec gravitational wave pulse; this is also the optimum length. The sensitivity is sufficient to detect putative events from distances up to the Virgo cluster.

Sampling permits extraction of signals even when the light spends one or more gravitational wave periods in the interferometer.

Unlike a Fabry-Perot cavity or a Herriot delay line where the light beam is recorded after it undergoes multiple reflections in a cavity, we note that the light beam is averaged, and recorded at the end of *each round-trip*. The sampled data stream is processed in accordance with algorithms used for over-sampled detection. The proposed design differs in this aspect from folded interferometers.

B. Proposed Design

Once we realize that the sensitivity is independent of L , the interferometer arms are chosen for convenience to be $10cm$ long; the design options also allow some flexibility. For one; a small interferometer is easier to build, easier to control the environment (temperature, pressure, isolation from external noise etc.). The entire interferometer can be mounted on

single platform. Sampling the signal at the end of every round-trip prevents the accumulation of excess phase by using the beams only once.

Mechanical stability is facilitated by mounting all the components on a 15cm diameter, 2cm thick sapphire disk. Sapphire is a suitable material because of its low thermal expansion coefficient ($\alpha \sim 10^{-6}/\text{C}^\circ$), excellent thermal conductivity ($0.4\text{watts}/\text{cmK}^\circ$), low mechanical dissipation ($Q \approx 10^9$, reduces Brownian noise), stiff Young's modulus ($\sim\text{GPa}$) and a high speed of sound (10^4m/s) [6], so a high fundamental vibration frequency which facilitates isolation from external vibrations.

1. Noise from Brownian motion and radiation pressure

We can estimate the Brownian noise contribution. The mirrors, which need be no more than 5mm in diameter; in order to maintain a high fundamental frequency, they may be sculpted directly into the sapphire disk. The entire platform vibrates due to thermal excitation. Far below the fundamental resonance at ω_0 its amplitude excursion is:

$$x_{rms}^B = \sqrt{\frac{4k_B T Q^{-1}}{\omega m \omega_0^2}} = \pm \frac{2.1 \times 10^{-18} \text{m}/\sqrt{\text{Hz}}}{\sqrt{\omega}} \quad (22)$$

for $T = 300\text{K}$, $Q \sim 10^6$, $m = 1\text{kg}$, $\omega_0 \approx 2\pi \times 10^4$. After p discrete samples each of interval τ_i , the average excursion is

$$x_{rms}^B = \sqrt{\frac{4k_B T Q^{-1}}{\omega m \omega_0^2}} \sqrt{\frac{1}{\tau_i}} \sqrt{\frac{1}{p}} = \sqrt{\frac{4k_B T Q^{-1}}{\omega m \omega_0^2}} \sqrt{\frac{c}{2L_i}} \sqrt{\frac{2L_i}{10^{-2}c}} = \pm \frac{1.2 \times 10^{-18} \text{m}}{\sqrt{\omega}} \quad (23)$$

x_{rms}^B depends on the total sampling interval, independent of the number of samples or the individual sampling interval. The time jitter due to Brownian motion is $\pm x_{rms}^B/c$:

$$x_{rms}^B/c = \pm \frac{4 \times 10^{-27} \text{secs}}{\sqrt{\omega}}$$

For the example under consideration the shot noise time jitter is Eq.(18)

$$\sigma_{\delta\tau} = \pm \sqrt{\frac{2\hbar\lambda}{P_{in}\pi c\tau_i}} \sqrt{\frac{1}{p}} = \pm 3.3 \times 10^{-24} \text{secs}$$

Brownian noise exceeds shot noise only when $\omega < 10^{-6}$.

Radiation pressure will also inject random vibrations in the mirrors. We propose using a laser of $P_{in} = 1\text{watt}$ and $\lambda = 0.545\mu\text{m}$. The amplitude excursion, for p discrete samples each of duration τ_i , appropriate for $\omega \ll \omega_0$ is:

$$x_{rms}^R = \frac{\omega}{m\omega_0^3} \sqrt{\frac{2\pi\hbar P_{in}}{c\lambda Q}} \sqrt{\frac{1}{\tau_i}} \sqrt{\frac{1}{p}} = \pm 2.9 \times 10^{-32} \text{m} \quad (24)$$

for $\omega_{\text{max}} = 2\pi \times 800$. The time uncertainty is:

$$x_{rms}^R/c = \pm 10^{-44} \text{secs}$$

Again this is negligible compared with the time uncertainty due to shot noise. Noise from Brownian motion and radiation pressure can be ignored.

It is worth repeating that the light beams reflect off each mirror only once, then they strike the photo-diode and are removed from the interferometer. Light from single reflections is corrupted by fluctuations in the mirror position due to radiation pressure and/or shot noise. Because each reflection is independent, the noise contributions are also independent. They add in quadrature. By contrast the situation in folded interferometers which utilize multiple reflections, is different because mirror noise fluctuations accumulate with each reflection, in practice limiting the number of folded beams [4].

C. Measurement Method

The photodiode detects interference fringes, actually a circular region which may be all shades from completely dark to completely bright. The photodiode output is sampled every nanosecond. To make data handling manageable, the photodiode output is fed first into an analogue integrator with a time constant which is a small fraction of the expected (reciprocal) signal frequency. For example a $10\mu\text{sec}$ time constant is sufficient for 125 samples of an 800Hz signal or 1000 samples of a 100Hz signal. Following the integrator the averaged signal is sent to a 16-bit analogue to digital converter and from there onto a library for comparison against different signal templates.

Referring to the earlier mention of a mode of operation Eq.(17), it turns out that refinements are needed to operate the interferometer as a null detector. Pockels cells need to be inserted to provide phase modulation. The interferometer operation point is moved to a dark fringe [3]. Because of the stiff mounting of the mirrors, it may be possible to maintain the dark fringe condition by further slow modulation of the Pockels cells.

The small size of the interferometer (diameter 15cm.) facilitates operation in a vacuum environment (10^{-7}T is sufficient for $h \approx 10^{-22}$); it also opens up several schemes to isolate it from seismic vibrations which is a major source of noise at low frequencies. Isolation from ground vibrations is made easier because the design fundamental mode is $\omega_0 = 2\pi \times 10^4$. This is one great advantage in using rigidly mounted mirrors and a high-Q platform.

The interferometer needs a laser source stabilized against both intensity and frequency drifts. Use of sapphire also minimizes platform distortions due to temperature inhomogeneities. Instruments will be needed to monitor and control the temperature.

The scheme described here can be extended to a three-axis detector, which may be replicated and installed as an antenna array on several optimal locations on Earth, sent into orbit, even mounted on the Moon.

Conclusion 1 *We have shown how use of signal processing techniques may allow a table-top 10cm Michelson interferometer sufficient sensitivity to detect gravitational waves from infalling binary neutron stars from as far as the Virgo cluster.*

Acknowledgments

We acknowledge with gratitude an anonymous referee for planting the seed of an idea, and M. Bocko for technical advice.

- [1] J. Weber, *General Relativity and Gravitational Waves*, (Interscience Publishers, New York, 1961)
- [2] G.E. Moss, L.R. Miller, R.L. Forward, *Appl. Optics*, **10**, 2495 (1971), R.L. Forward, *Phys. Rev. D***17**, 379 (1978)
- [3] R. Weiss, *MIT Quart. Prog. Rep.* **105**, 54 (1972)
- [4] P.R. Saulson, *Fundamentals of Interferometric Gravitational Wave Detectors*, (World Scientific, Singapore, 1994)
- [5] <http://www.ligo.caltech.edu>
- [6] <http://www.saphikon.com>
- [7] K. S. Thorne in *300 Years of Gravitation*, Eds. S. Hawking and W. Israel, (Cambridge University Press, 1987)
- [8] J.L. Martin, *General Relativity*, (Prentice Hall, 1988, 1996)
- [9] C.W. Misner, K.S. Thorne and J.A. Wheeler, *Gravitation*, p. 63 (W.H. Freeman, San Francisco, 1973)
- [10] H.J. Hay, J.P. Schiffer and P.A. Egelstaff, *Phys. Rev. Lett.* **4**, 165 (1960), W. Kündig, *Phys. Rev.* **129**, 2371 (1963), D.C. Champeney, G. R. Isaak and A.M. Khan, *Phys. Lett.* **7**, 241 (1963), G.R. Isaak, *Phys. Bull.* **21**, 255 (1970). There was an experiment performed where relativistic muons were slammed into a beam dump. The enormous deceleration was meant to simulate a strong gravity field which would presumably slow down the muon decay rate. No general relativistic effects were observed, only the usual time dilation expected from special relativity; confirming that acceleration is not a substitute for gravity. Unfortunately I haven't been able to find the reference.
- [11] K. Green, private communication

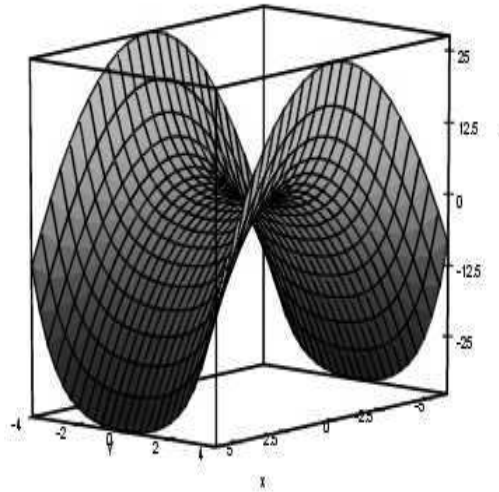


FIG. 1: Surface of gravity wave-front. Shown is the field amplitude $h_{\mu\nu}$ along the z -axis: at this instant h_{11} is along the x -axis and h_{22} is along the y -axis. The surface has intrinsic curvature. An excess phase appears in a null vector parallel transported in a circuit on this surface. $\Delta\phi_i$ is the difference in excess phase between a circuit along the x - and y -axes.

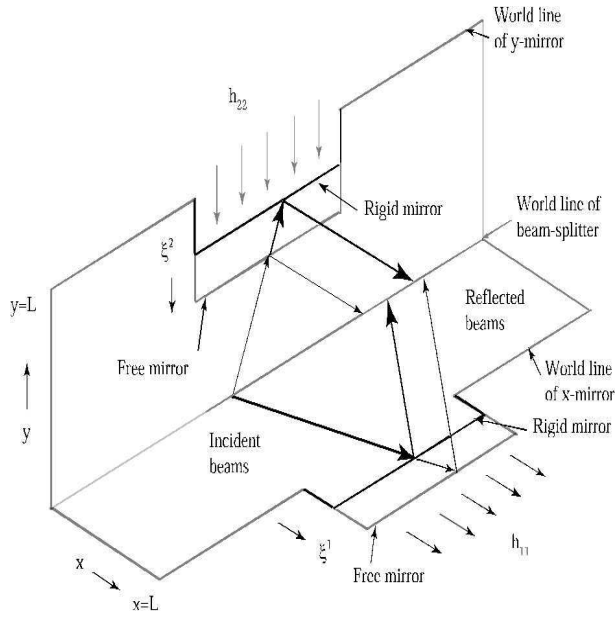
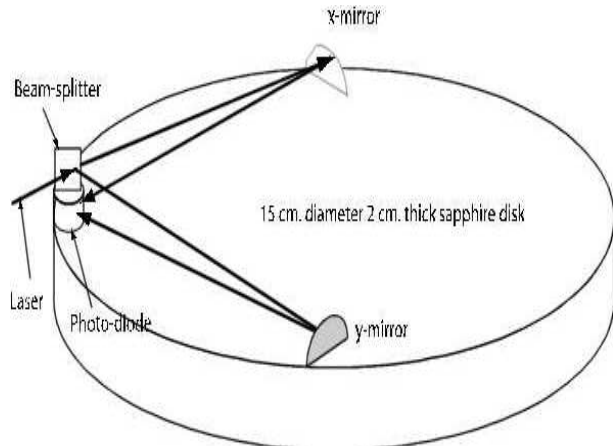


FIG. 2: World lines of rays and interferometer components. Two mirror mounts, free in light and rigid in heavy lines, are shown under the influence of a gravity wave of amplitude $h_{\mu\nu}$. Although the surfaces are shown as planes they are saddle-shaped as in figure 1. The reflection points depend on the type of mirror mount, and so does the excess phase.



Sampled gravity wave interferometer

FIG. 3: Schematic arrangement of interferometer components. Coherent beams reflect off the x - and y -mirrors, when they strike the photo-diode they exit the interferometer. Output is sampled in discrete intervals: the intensity pattern is reconstructed using sampling algorithms. Each sample is independent.